
Development of Solution-Processed p-Type Polycrystalline SnSe Thermoelectric Nanomaterials

Journal:	<i>Materials Lab</i>
Manuscript ID	MATLAB-2024-0008.R1
Manuscript Type:	Perspective
Date Submitted by the Author:	22-Nov-2024
Complete List of Authors:	Lu, Shaoqing; Hefei University of Technology Huang, Lulu; Hefei University of Technology Liu, Yu; Hefei University of Technology
Keywords:	Thermoelectric, Solution processing, Tin selenide
Speciality:	Thermoelectrics

SCHOLARONE™
Manuscripts

Development of Solution-Processed p-Type Polycrystalline SnSe Thermoelectric Nanomaterials

Shaoqing Lu,^a Lulu Huang,^b Yu Liu^{a,*}

^a School of Chemistry and Chemical Engineering, Hefei University of Technology, 230009, Hefei, China.

^b School of Materials Science and Engineering, Hefei University of Technology, Hefei 230009, China.

* E-mail: yliu@hfut.edu.cn

This article has been accepted for publication and undergone full peer review but has not been through the copyediting, typesetting, pagination and proofreading process, which may lead to differences between this version and the Version of Record.

Accepted Article
For Review Only

Abstract: SnSe has emerged as a promising mid-temperature thermoelectric (TE) material, noted for its intrinsically low lattice thermal conductivity and favorable electronic properties. Solution-processing provides a scalable and adaptable approach to synthesizing polycrystalline SnSe, allowing for precise control over nanostructure, defect density, and dopant distribution, which are essential factors in optimizing TE performance. Advances in doping/alloying, defect engineering and surface functionalization have been shown to enhance carrier concentrations, Seebeck coefficients, and reduced lattice thermal conductivity in p-type SnSe, resulting in notable TE efficiency. However, achieving comparable efficiency in solution-processed n-type SnSe remains challenging due to limited electron carrier concentration. In addition, Additionally, low carrier mobility further limits the TE performance of polycrystalline SnSe at low temperatures. This perspective briefly explores the development of solution-processed SnSe nanostructures, with a focus on ongoing advancements in processing techniques and optimization strategies essential for promotingadvancing solution-processed SnSe toward practical TE applications.

Key words: Thermoelectric; Solution processing; Tin selenide

1
2
3
4 Thermoelectric (TE) materials enable the direct and reversible conversion of heat into
5
6 electricity, making them highly valuable for applications in clean energy, aerospace technology,
7
8 and solid-state cooling. TE devices consist of multiple p-type and n-type inorganic
9
10 semiconductors, which are composed of multiple p-type and n-type inorganic
11
12 semiconductors arranged electrically in series and thermally in parallel to form an all-solid-
13
14 state module^[1]. The efficiency of TE devices is determined by the figure of merit (zT), which
15
16 integrates the Seebeck coefficient (S), electrical conductivity (σ), and thermal conductivity (κ).
17
18 Achieving high zT values requires a precise balance of these properties, thereby enhancing High
19
20 zT values are achieved by carefully balancing these properties, resulting in improved energy
21
22 conversion efficiency^[2,3].
23
24
25
26
27
28
29

30 SnSe has become as a promising candidate for medium-temperature TE applications,
31
32 owing attributed to its unique layered structure and excellent TE properties^[4,5]. In 2014, Zhao *et*
33
34 *al.* first reported the ultralow thermal conductivity and high figure of merit zT in single-
35
36 crystalline SnSe, this material has consistently demonstrated remarkable zT values along
37
38 specific crystallographic directions^[6]. These outstanding properties are primarily attributed to
39
40 its intrinsically low lattice thermal conductivity (κ_L) and favorable electronic characteristics^[7].
41
42
43
44

45 The application of single-crystal SnSe has been constrained by high production costs and
46
47 challenges in mechanical stability^[4]. Thus, polycrystalline SnSe provides a mechanically robust
48
49 alternative with the potential for scalable production. However, polycrystalline SnSe
50
51 synthesized via both solution-based^[8-30] and solid-state^[31-43] methods often exhibits carrier
52
53 mobility that is often reduced by an order of magnitude compared to single crystals (Figure
54
55 1a)^[6]. This reduction is primarily caused by strong carrier scattering at closely arranged grain
56
57
58
59
60

boundaries and surface oxidation at grain interfaces, which together lead to lower σ , particularly at low temperatures, and higher κ compared to SnSe crystals^[4,44]. To enhance the TE performance of polycrystalline SnSe and address existing challenges, strategies including stoichiometry control^[8,9,11,12,16], doping/alloying^[10,13,15,17,18,20,22–26,31–38,40–43], nanocomposites (NCPs) formation^[14,19,21,28,29], and surface oxide removal have been applied^[39,45], leading to significant improvements in zT values for materials produced by both solid-state and solution-processed methods.

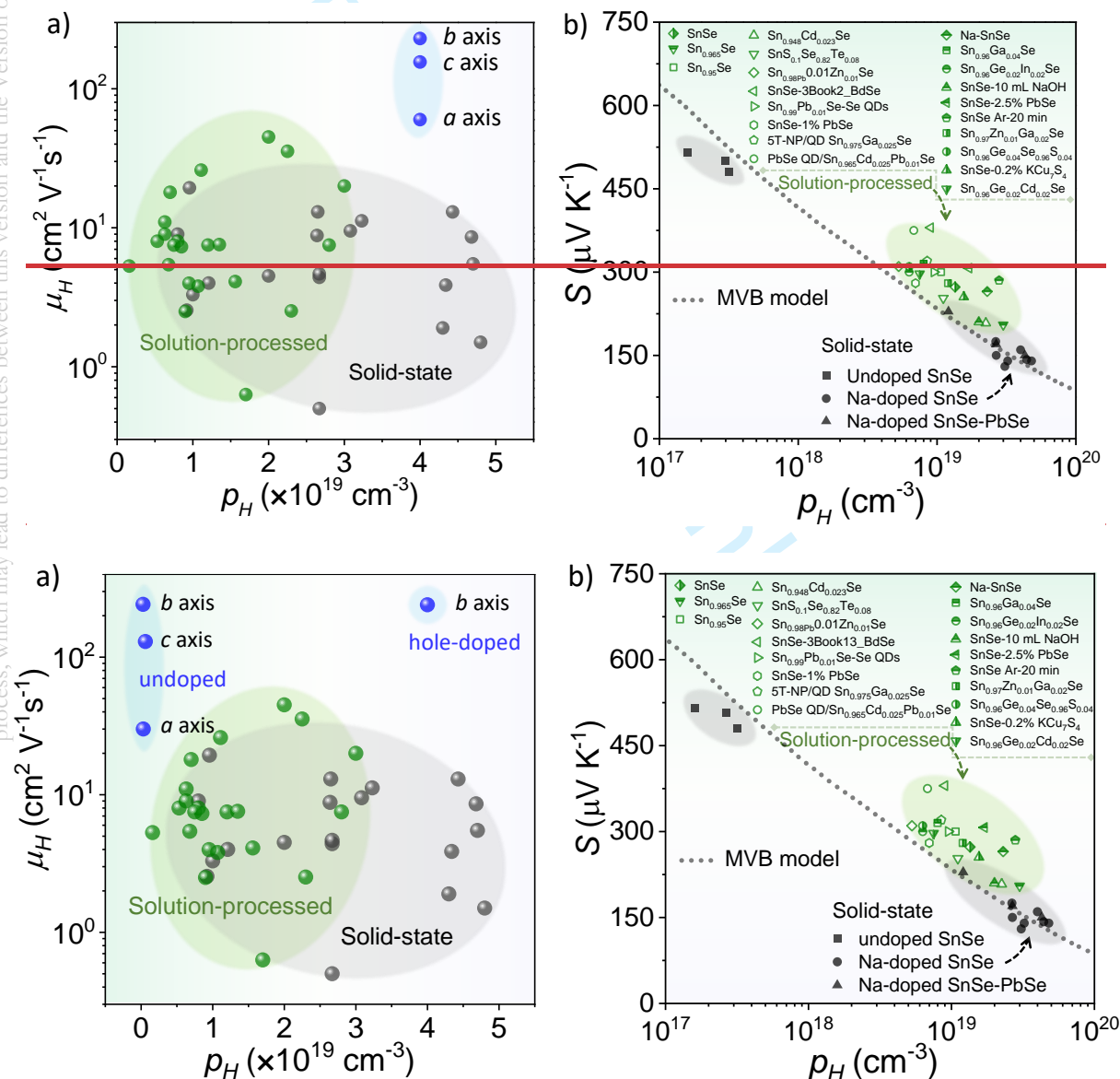


Figure 1. (a) Hall mobility (μ_H) of p-type polycrystalline SnSe as a function of hole concentration (p_H) for solution-processed (green dots)^[8–30], solid-state (gray dots)^[31–43], and single-crystal SnSe (blue dots)^[6,46]. (b) Pisarenko plot at 300 K, with green symbols representing solution-processed materials^[8–22,24–30] and black symbols denoting solid-state synthetic methods^[31,35–40], including single crystals^[6,46]. The dashed line was calculated using a multiple band model^[47].

In comparison to solid-phase methods, solution-processing provides a cost-effective and scalable approach that allows precise control over material morphology, grain size, composition, and crystalline structure, while traditional solid-state synthesis requires high temperatures and substantial energy^[1]. ~~The control available~~~~This control~~ in solution-processed SnSe enables the formation of specific nanostructural features, *i.e.*, defect engineering, grain boundary construction, and optimized dopant distribution, which are essential for improving phonon scattering and thus enhancing TE properties, ultimately ~~providing~~~~offering~~ distinct advantages in tailoring overall performance. Additionally, this technique allows for the incorporation of various dopants and secondary phases, providing a versatile approach for optimizing both carrier concentration and mobility^[48]. Therefore, while polycrystalline SnSe-based TE materials prepared by solution-processing methods exhibit slightly lower carrier concentrations than those produced by solid-state techniques (Figure 1a), the comparable carrier mobility and reduced κ_L contribute to enhanced TE performance.

Initially, SnSe attracted ~~sed~~ attention as a key p-type IV-VI semiconductor due to its nearly optimal bandgap for photovoltaic applications, before being recognized as a promising TE

1
2
3
4 material, with synthetic approaches primarily using colloidal methods that, despite their ability
5
6 to produce high-quality SnSe nanocrystals (NCs) in various morphologies including nanostars,
7
8 nanowires, nanoflowers, and nanosheets, face significant limitations in scalability and practical
9
10 application resulting from their reliance on TOP-Se, a highly toxic and expensive
11
12 trioctylphosphine-based precursor^[49–51]. This limitation has directed researchers toward
13
14 hydrothermal/solvothermal^[8,9,21,23,24,26,27,29,30,10–12,15–18,20], and aqueous solution-based synthesis
15
16 methods^[13,14,19,22,25,28,52], which provide safer, more economically feasible alternatives for large-
17
18 scale production by reducing the dependence on toxic reagents, thereby ~~facilitating~~ supporting
19
20 the scalable development of TE materials. The production of surfactant-free SnSe
21
22 nanomaterials typically involves polar solvents, such as water or ethylene glycol, in
23
24 hydrothermal/solvothermal methods, or is ~~carried out~~ conducted in aqueous solution-based
25
26 methods at atmospheric pressure in boiling water. These reactions commonly employ sodium-
27
28 containing compounds, including NaBH₄, NaOH, and Na₂SeO₃, *etc.* as redox agents and
29
30 acid/base additives^[8–30]. Compared to conventional hydrothermal and solvothermal methods,
31
32 aqueous solution-based approaches present notable advantages by minimizing the reliance on
33
34 specialized reaction vessels and conditions, enhancing economic efficiency, and providing
35
36 significant potential for large-scale production.
37
38
39
40
41
42
43
44
45
46
47
48
49
50
51
52
53
54
55
56
57
58
59
60

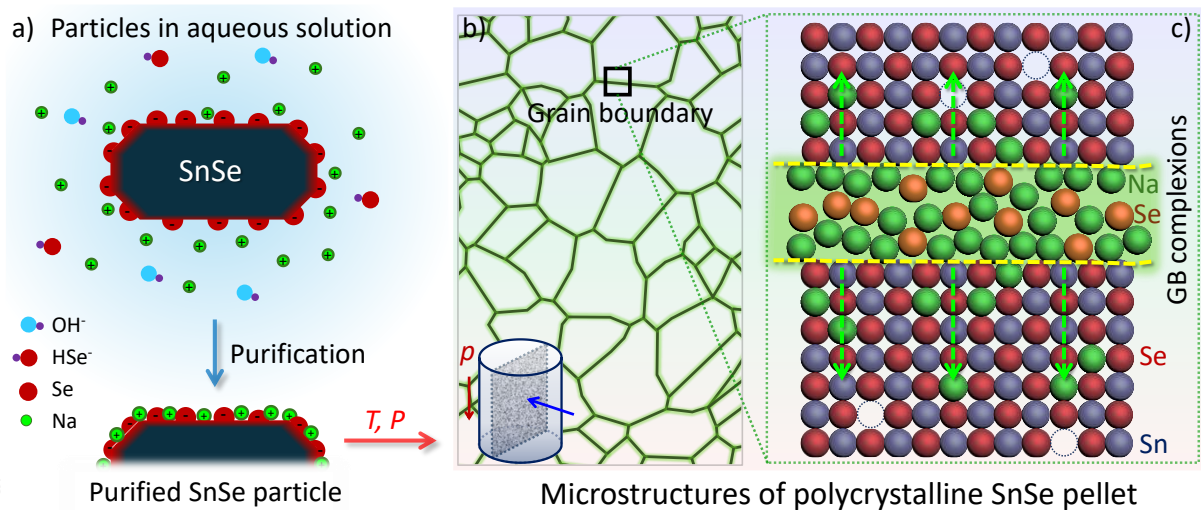


Figure 2. (a) Schematic representation of a SnSe particle in aqueous solution, with Na⁺ ions adsorbed to maintain charge neutrality after purification^[13]. (b) Diagram of the grain boundary interface in aqueous-synthesized SnSe after thermal annealing and sintering. (c) Enlarged view of the grain boundary (GB), showing the complexes and atomic diffusion mechanisms within the matrix of the system.

Surfactant-free SnSe particles synthesized by via aqueous solution methods exhibit high σ and S after consolidation, while maintaining relatively low κ_L , a combination that enables superior TE performance without requiring intentional doping. Compared to SnSe produced via conventional solid-state methods, this method yields samples with significantly high carrier concentrations ($>2 \times 10^{19} \text{ cm}^{-3}$), a characteristic attributed in previous studies not solely to intrinsic Sn vacancies^[13,53]. The aqueous solution synthesis process involves alternating purification steps with solvents of different polarities, such as water and ethanol, which are essential for controlling composition and optimizing performance. Our recent studies have thoroughly examined the critical chemical processing steps involved in the solution-based

1
2
3
4 synthesis of SnSe, including particle synthesis, purification, annealing, and consolidation^[53].
5
6 During these steps, residual Na⁺ ions, electrostatically adsorbed onto the negatively charged
7
8 surfaces of SnSe particles, remain partially unremovable through purification and subsequently
9
10 combine with excess Se on the particle surface to form Na₂Se_x phases^[13]. Upon annealing in
11
12 forming gas (95% N₂+ 5% H₂) and subsequent consolidation, these low-melting Na₂Se_x phases
13
14 facilitate microstructural optimization^[54,55], significantly enhancing TE transport properties by
15
16 increasing carrier concentration and enhancing the *S* through the energy-filtering effect at grain
17
18 boundary barriers. Furthermore, the Pisarenko plot reveals that most solution-processed SnSe
19
20 samples (green symbols) exhibit *S* values exceeding the expected values, a trend not observed
21
22 in Na-doped solid-state synthesized SnSe samples (black symbols, including single crystals),
23
24 as shown in Figure 1b. Na⁺ ions ultimately stabilize within bulk SnSe in two distinct forms: i)
25
26 as partial substitutes for Sn²⁺ within the lattice, acting as p-type dopants; and ii) at grain
27
28 boundaries and defects, accumulating during sintering to form Na-enriched interfacial
29
30 complexions or precipitates at grain boundaries (Figure 2). Therefore, the influence of surface
31
32 adsorbates requires careful consideration, especially when alkali metal salts or hydroxides (such
33
34 as Li⁺ or K⁺, in addition to Na⁺) are employed as reactants in solution-based synthesis. Precise
35
36 control over the purification, thermal annealing treatment, and sintering processes of SnSe
37
38 particles is crucial, accompanied by detailed documentation of these steps in the experimental
39
40 section to ensure reproducibility^[53].
41
42
43
44
45
46
47
48
49
50
51
52

53 While theis solution-processed p-type SnSe bulk materials have achieved ideal carrier
54
55 concentration levels (10¹⁹ cm⁻³) and exhibit superior TE performance, it is notable that n-type
56
57 SnSe synthesized via aqueous or other solution-based methods shows considerably lower TE
58
59
60

1
2
3
4 efficiency in comparison to its p-type SnSe. Despite increasing the content of n-type dopants,
5
6 achieving a substantial enhancement in electron carrier concentration remains challenging^[22,56].
7

8
9 We believe this is correlated to the fact that all synthetic methods use of alkali metal Na salts in
10
11 the preparation of SnSe particles, where the presence of Na induces a pinning effect when n-
12
13 type dopants are introduced and is further supported by the fact that all reported high-
14
15 performance n-type polycrystalline SnSe materials ($zT > 2$) have been synthesized through solid-
16
17 state methods^[57–60]. Therefore, to develop high-performance n-type polycrystalline SnSe
18
19 through solution-processed methods, avoiding the use of alkali metal salts or alkali hydroxides
20
21 is recommended, with alternative reagents, *e.g.*, tetramethylammonium salts and ascorbic acid,
22
23 serving as potential substitutes.
24
25
26
27
28
29

30 Moreover, we suggest that for p-type SnSe particles synthesized via aqueous solution
31
32 methods with alkali metal compounds as reactants, efforts to improve electrical transport
33
34 properties through doping/alloying are often ineffective, with these strategies potentially further
35
36 reducing the already low carrier mobility of the polycrystalline SnSe, leading to an additional
37
38 decrease in σ , especially at low temperatures. For example, during the alloying process where
39
40 surfactant-free SnSe particles are combined with colloidal PbSe NCs to form SnSe-PbSe NCPs
41
42 some Na⁺ ions electrostatically adsorbed on the surfaces of the SnSe particles interact with the
43
44 oleate capping ligands on PbSe NCs, forming Na-oleate, which is subsequently removed
45
46 through particle purification^[14].
47
48
49
50
51
52
53
54
55
56
57
58
59
60

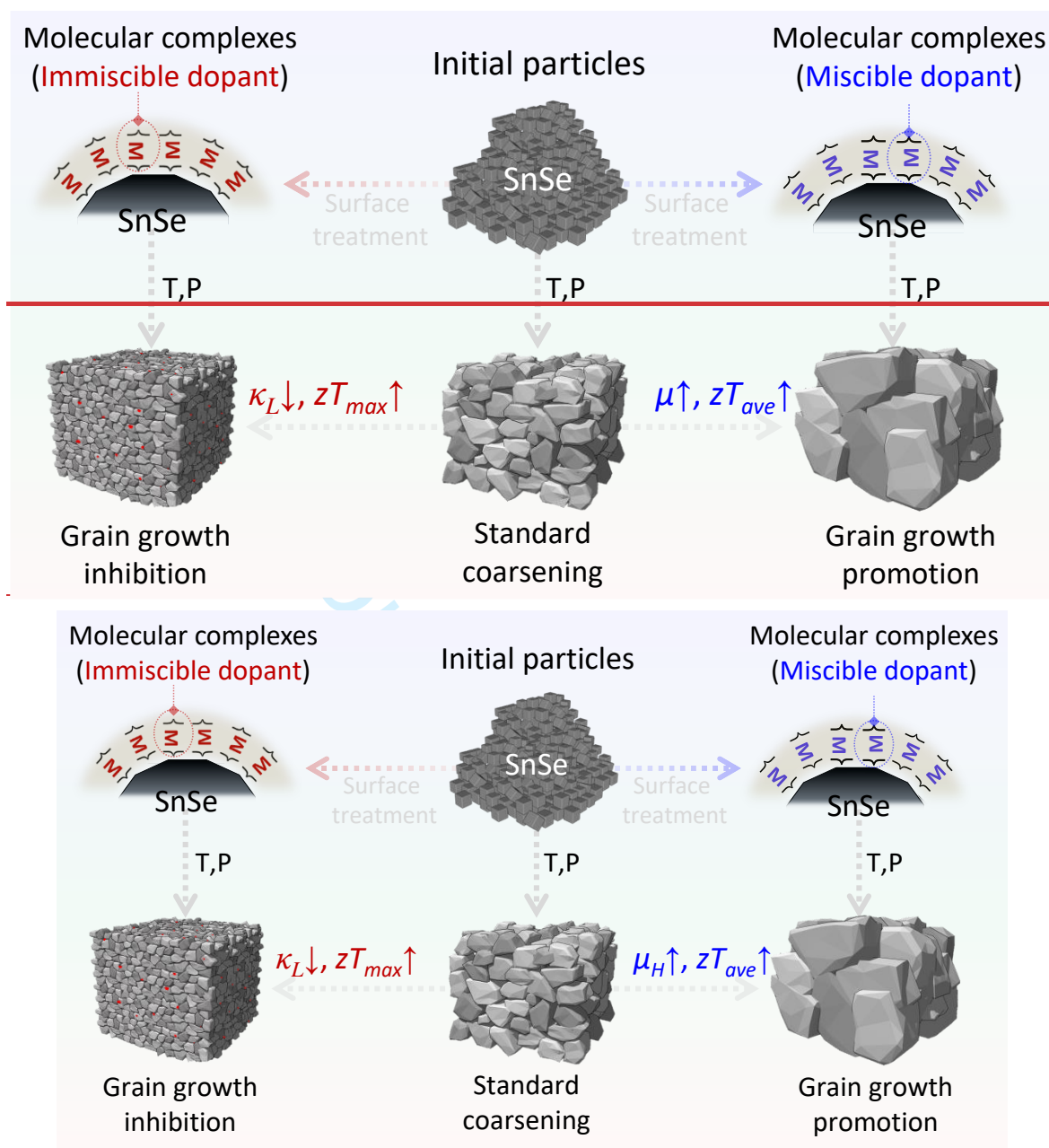


Figure 3. Schematic of crystal domain growth during the annealing and consolidation of SnSe particles under conditions without and with different types of molecular complexes.

The surface functionalization of SnSe particles with CdSe molecular complexes, prepared in an “amine-thiol” solution, results in SnSe-CdSe NCPs in which CdSe remains insoluble within the SnSe matrix across the entire operating temperature range. CdSe nanoprecipitates

1
2
3
4 are uniformly distributed within the SnSe matrix, creating a high density of grain boundaries
5
6 through a Zener pinning effect that inhibits significant grain growth in SnSe-CdSe samples
7
8 during thermal processing, thereby preserving the dimensional advantages characteristic of
9
10 low-dimensional nanostructured TE materials^[28,61]. With coordinated control of dislocations
11
12 and multiscale defects, this structure effectively reduces the κ_L of the NCPs. Simultaneously,
13
14 the consistent level of unavoidable Na impurities during the surface treatment of polycrystalline
15
16 SnSe maintains electrical properties, significantly enhancing its high-temperature TE
17
18 performance, yielding a zT of 2.2 at 786 K. This approach is particularly effective for systems
19
20 with high carrier concentrations, such as SnTe, Cu_{2-x}Te and Ag_2Se -based materials^[62,63], that
21
22 seek to maximize TE performance (zT_{max}) in the mid-to-high temperature range by reducing κ_L .
23
24 For materials requiring a high average thermoelectric figure of merit (zT_{ave}) across low-
25
26 temperature ranges, enhancing carrier mobility through grain boundary engineering and
27
28 optimized doping mechanisms is essential, as is identifying molecular complexes compatible
29
30 with the SnSe matrix that effectively function as “solders” mutually soluble with the
31
32 matrix. However, for materials requiring a high average TE figure of merit (zT_{ave}) across low
33
34 temperature range, it is essential to identify molecular complexes compatible with the SnSe
35
36 matrix, effectively functioning as “solder” that are mutually soluble with the matrix^[64]. These
37
38 “solder” complexes, when applied to the SnSe particle surface, facilitate atomic diffusion into
39
40 the grains during high-temperature treatment, thereby promoting solid solution formation,
41
42 accelerating grain boundary migration, and inducing grain growth. This process reduces grain
43
44 boundary barriers and enhances carrier mobility in polycrystalline SnSe at low-temperature
45
46 range (Figure 3)^[2,65–68]. However, identifying compatible systems and optimizing post-
47
48
49
50
51
52
53
54
55
56
57
58
59
60

1
2
3
4 treatment conditions based on the phase diagrams of SnSe and related compounds remains
5
6 challenging.

7
8
9 In this perspective, ~~the strategies discussed above~~~~these above strategies~~ provide valuable
10
11 insights into the transport mechanisms of TE materials and open new avenues for the controlled
12
13 synthesis of advanced polycrystalline SnSe-based TE nanostructures. Solution-processed SnSe
14
15 demonstrates ~~significant~~~~considerable~~ potential for high TE performance through defect and
16
17 surface engineering; ~~however, further optimization remains crucial for advancing solution-~~
18
19 ~~processed SnSe toward practical applications, with key improvements including refining~~
20
21 ~~solution-processing conditions to achieve greater reproducibility, enhancing material stability~~
22
23 ~~against oxidation, and optimizing carrier mobility~~~~however, further investigation into process~~
24
25 ~~optimization is essential to advance solution-processed SnSe toward practical applications.~~
26
27
28
29
30
31
32
33
34
35

36 **Acknowledgements**

37
38 Y.L. acknowledges funding from the National Natural Science Foundation of China (NSFC)
39
40 (Grants No. 22209034), the Innovation and Entrepreneurship Project of Overseas Returnees in
41
42 Anhui Province (Grant No. 2022LCX002) and the Fundamental Research Funds for the Central
43
44 Universities (JZ2024HGTA0179). L.H. acknowledges the Fundamental Research Funds for the
45
46 Central Universities (JZ2023HGTA0179).
47
48
49
50
51

52 **Conflict of interest**

53
54
55
56 The authors declare no conflict of interest.
57
58
59
60

REFERENCES

- [1] S. Ortega, M. Ibáñez, Y. Liu, Y. Zhang, M. V. Kovalenko, D. Cadavid, A. Cabot, *Chem. Soc. Rev.* 2017, 46, 3510.
- [2] B. Qin, L.D. Zhao, *Mater. Lab* 2022, 1, 220004.
- [3] Y. Xiao, *Mater. Lab* 2022, 1, 220025.
- [4] L. D. Zhao, C. Chang, G. Tan, M. G. Kanatzidis, *Energy Environ. Sci.* 2016, 9, 3044.
- [5] **D. Liu, B. Qin, L.D. Zhao, *Mater. Lab* 2022, 1, 220006.**
- [6] L. D. Zhao, S. H. Lo, Y. Zhang, H. Sun, G. Tan, C. Uher, C. Wolverton, V. P. Dravid, M. G. Kanatzidis, *Nature* 2014, 508, 373.
- [7] Y. Xiao, C. Chang, Y. Pei, D. Wu, K. Peng, X. Zhou, S. Gong, J. He, Y. Zhang, Z. Zeng, L.D. Zhao, *Phys. Rev. B* 2016, 94, 125203.
- [8] W. Wei, C. Chang, T. Yang, J. Liu, H. Tang, J. Zhang, Y. Li, F. Xu, Z. Zhang, J.-F. Li, G. Tang, *J. Am. Chem. Soc.* 2017, 140, 499.
- [9] X. Shi, Z. G. Chen, W. Liu, L. Yang, M. Hong, R. Moshwan, L. Huang, J. Zou, *Energy Storage Mater.* 2018, 10, 130.
- [10] Y. Gong, S. Zhang, Y. Hou, S. Li, C. Wang, W. Xiong, Q. Zhang, X. Miao, J. Liu, Y. Cao, *ACS Nano* 2022, 17, 801.
- [11] X. Shi, W. Liu, A. Wu, V. T. Nguyen, H. Gao, Q. Sun, R. Moshwan, J. Zou, Z. Chen, *InfoMat* 2020, 2, 1201.
- [12] X.-L. Shi, W.-D. Liu, M. Li, Q. Sun, S.-D. Xu, D. Du, J. Zou, Z.-G. Chen, *Adv. Energy Mater.* 2022, 12, 2200670.
- [13] Y. Liu, M. Calcabrini, Y. Yu, A. Genç, C. Chang, T. Costanzo, T. Kleinhanns, S. Lee, J. Llorca, O. Cojocar-Mirédin, M. Ibáñez, *Adv. Mater.* 2021, 33, 2106858.
- [14] Y. Liu, S. Lee, C. Fiedler, M. Chiara Spadaro, C. Chang, M. Li, M. Hong, J. Arbiol, M. Ibáñez, *Chem. Eng. J.* 2024, 490, 151405.
- [15] S. Li, X. Lou, B. Zou, Y. Hou, J. Zhang, D. Li, J. Fang, T. Feng, D. Zhang, Y. Liu, *Mater. Today Phys.* 2021, 21, 100542.
- [16] C. Wu, X. Shi, M. Li, Z. Zheng, L. Zhu, K. Huang, W. Liu, P. Yuan, L. Cheng, Z. Chen, *Adv. Funct. Mater.* 2024, 34, 2402317.

- 1
2
3
4 [17] S. Li, Y. Hou, D. Li, B. Zou, Q. Zhang, Y. Cao, G. Tang, *J. Mater. Chem. A* 2022, 10,
5 12429.
6
7 [18] Y. Gong, P. Ying, Q. Zhang, Y. Liu, X. Huang, W. Dou, Y. Zhang, D. Li, D. Zhang, T.
8 Feng, *Energy Environ. Sci.* 2024, 17, 1612.
9
10 [19] X. Liu, Y. Chen, H. Wang, S. Liu, B. Zhang, X. Lu, G. Wang, G. Han, X. Chen, X. Zhou,
11 *ACS Appl. Mater. Interfaces* 2024, 16, 2240.
12
13 [20] X. Lou, S. Li, X. Chen, Q. Zhang, H. Deng, J. Zhang, D. Li, X. Zhang, Y. Zhang, H.
14 Zeng, G. Tang, *ACS Nano* 2021, 15, 8204.
15
16 [21] W. Dou, Y. Gong, X. Huang, Y. Li, Q. Zhang, Y. Liu, Q. Xia, Q. Jian, D. Xiang, D. Li,
17 D. Zhang, S. Zhang, P. Ying, G. Tang, *Small* 2024, 20, 2311153.
18
19 [22] X. Li, C. Chen, W. Xue, S. Li, F. Cao, Y. Chen, J. He, J. Sui, X. Liu, Y. Wang, Q. Zhang,
20 *Inorg. Chem.* 2018, 57, 13800.
21
22 [23] Z.-C. Wang, X.-D. Jiang, Y.-X. Duan, X. Wang, Z.-H. Ge, J.-M. Cai, X.-M. Cai, H.-L.
23 Tan, *J. Eur. Ceram. Soc.* 2024, 44, 1636.
24
25 [24] X. Shi, A. Wu, T. Feng, K. Zheng, W. Liu, Q. Sun, M. Hong, S. T. Pantelides, Z.-G.
26 Chen, J. Zou, *Adv. Energy Mater.* 2019, 9, 1803242.
27
28 [25] L. Huang, G. Han, B. Zhang, D. H. Gregory, *J. Mater. Chem. C* 2019, 7, 7572.
29
30 [26] J. J. Liu, P. Wang, M. Wang, R. Xu, J. Zhang, J. J. Liu, D. Li, N. Liang, Y. Du, G. Chen,
31 G. Tang, *Nano Energy* 2018, 53, 683.
32
33 [27] R. Xu, L. Huang, J. Zhang, D. Li, J. Liu, J. Liu, J. Fang, M. Wang, G. Tang, *J. Mater.*
34 *Chem. A* 2019, 7, 15757.
35
36 [28] Y. Liu, M. Calcabrini, Y. Yu, S. Lee, C. Chang, J. David, T. Ghosh, M. C. Spadaro, C.
37 Xie, O. Cojocaru-Mirédin, J. Arbiol, M. Ibáñez, *ACS Nano* 2022, 16, 78.
38
39 [29] G. Tang, W. Wei, J. Zhang, Y. Li, X. Wang, G. Xu, C. Chang, Z. Wang, Y. Du, L. D.
40 Zhao, *J. Am. Chem. Soc.* 2016, 138, 13647.
41
42 [30] S. Li, Y. Hou, S. Zhang, Y. Gong, S. Siddique, D. Li, J. Fang, P. Nan, B. Ge, G. Tang,
43 *Chem. Eng. J.* 2023, 451, 138637.
44
45 [31] T. R. Wei, G. Tan, X. Zhang, C. F. Wu, J. F. Li, V. P. Dravid, G. J. Snyder, M. G.
46 Kanatzidis, *J. Am. Chem. Soc.* 2016, 138, 8875.
47
48
49
50
51
52
53
54
55
56
57
58
59
60

- 1
2
3
4 [32] T. R. Wei, C. F. Wu, X. Zhang, Q. Tan, L. Sun, Y. Pan, J. F. Li, *Phys. Chem. Chem.*
5 *Phys.* 2015, 17, 30102.
6
7 [33] C.-C. Lin, R. Lydia, J. Hyun Yun, H. Seong Lee, J. Soo Rhyee, *Chem. Mater.* 2017, 29,
8 5344.
9
10 [34] B. Su, Z. Han, Y. Jiang, H.-L. Zhuang, J. Yu, J. Pei, H. Hu, J.-W. Li, Y.-X. He, B.-P.
11 Zhang, J.-F. Li, *Adv. Funct. Mater.* 2023, 33, 2301971.
12
13 [35] E. K. Chere, Q. Zhang, K. Dahal, F. Cao, J. Mao, Z. Ren, *J. Mater. Chem. A* 2016, 4,
14 1848.
15
16 [36] Y. Luo, S. Cai, X. Hua, H. Chen, Q. Liang, C. Du, Y. Zheng, J. Shen, J. Xu, C. Wolverton,
17 V. P. Dravid, Q. Yan, M. G. Kanatzidis, *Adv. Energy Mater.* 2019, 9, 1803072.
18
19 [37] B. Cai, J. Li, H. Sun, P. Zhao, F. Yu, L. Zhang, D. Yu, Y. Tian, B. Xu, *J. Alloys Compd.*
20 2017, 727, 1014.
21
22 [38] Z. H. Ge, D. Song, X. Chong, F. Zheng, L. Jin, X. Qian, L. Zheng, R. E. Dunin-
23 Borkowski, P. Qin, J. Feng, L. D. Zhao, *J. Am. Chem. Soc.* 2017, 139, 9714.
24
25 [39] Y. K. Lee, Z. Luo, S. P. Cho, M. G. Kanatzidis, I. Chung, *Joule* 2019, 3, 719.
26
27 [40] Q. Zhao, D. Wang, B. Qin, G. Wang, Y. Qiu, L. D. Zhao, *J. Solid State Chem.* 2019, 273,
28 85.
29
30 [41] Y. X. Chen, Z. H. Ge, M. Yin, D. Feng, X. Q. Huang, W. Zhao, J. He, *Adv. Funct. Mater.*
31 2016, 26, 6836.
32
33 [42] S. Liang, J. Xu, J. G. Noudem, H. Wang, X. Tan, G.-Q. Liu, H. Shao, B. Yu, S. Yue, J.
34 Jiang, *J. Mater. Chem. A* 2018, 6, 23730.
35
36 [43] Q. Zhao, B. Qin, D. Wang, Y. Qiu, L.-D. Zhao, *ACS Appl. Energy Mater.* 2019, 3, 2049.
37
38 [44] A. K. Munirathnappa, H. Lee, I. Chung, *Mater. Lab* 2023, 2, 220056.
39
40 [45] C. Zhou, Y. K. Lee, Y. Yu, S. Byun, Z.-Z. Luo, H. Lee, B. Ge, Y.-L. Lee, X. Chen, J. Y.
41 Lee, O. Cojocar-Mirédin, H. Chang, J. Im, S.-P. Cho, M. Wuttig, V. P. Dravid, M. G.
42 Kanatzidis, I. Chung, *Nat. Mater.* 2021, 20, 1378.
43
44 [46] L.-D. Zhao, G. Tan, S. Hao, J. He, Y. Pei, H. Chi, H. Wang, S. Gong, H. Xu, V. P. Dravid,
45 C. Uher, G. J. Snyder, C. Wolverton, M. G. Kanatzidis, *Science* 2016, 351, 141.
46
47 [47] G. Shi, E. Kioupakis, *J. Appl. Phys.* 2015, 117, 065103.
48
49
50
51
52
53
54
55
56
57
58
59
60

- 1
2
3
4 [48] C. Fiedler, T. Kleinhanns, M. Garcia, S. Lee, M. Calcabrini, M. Ibáñez, *Chem. Mater.*
5 2022, 34, 8471.
6
7 [49] L. Li, Z. Chen, Y. Hu, X. Wang, T. Zhang, W. Chen, Q. Wang, *J. Am. Chem. Soc.* 2013,
8 135, 1213.
9
10 [50] X. Liu, Y. Li, B. Zhou, X. Wang, A. N. Cartwright, M. T. Swihart, *Chem. Mater.* 2014,
11 26, 3515.
12
13 [51] S. Liu, X. Guo, M. Li, W. H. Zhang, X. Liu, C. Li, *Angew. Chemie Int. Ed.* 2011, 50,
14 12050.
15
16 [52] G. Han, S. R. Popuri, H. F. Greer, J. W. G. Bos, W. Zhou, A. R. Knox, A. Montecucco,
17 J. Siviter, E. A. Man, M. MacAuley, D. J. Paul, W. G. Li, M. C. Paul, M. Gao, T. Sweet,
18 R. Freer, F. Azough, H. Baig, N. Sellami, T. K. Mallick, D. H. Gregory, *Angew. Chemie*
19 *Int. Ed.* 2016, 55, 6433.
20
21 [53] C. Fiedler, M. Calcabrini, Y. Liu, M. Ibáñez, *Angew. Chemie Int. Ed.* 2024, 63,
22 e202402628.
23
24 [54] J. Sangster, A. D. Pelton, *J. Phase Equilib.* 1997, 18, 185.
25
26 [55] S.-J. L. Kang, *Sintering: Densification, Grain Growth, and Microstructure*, Butterworth–
27 Heinemann, Oxford 2005.
28
29 [56] G. Han, S. R. Popuri, H. F. Greer, L. F. Llin, J.-W. G. Bos, W. Zhou, D. J. Paul, H.
30 Ménard, A. R. Knox, A. Montecucco, J. Siviter, E. A. Man, W. Li, M. C. Paul, M. Gao,
31 T. Sweet, R. Freer, F. Azough, H. Baig, T. K. Mallick, D. H. Gregory, *Adv. Energy Mater.*
32 2017, 7, 1602328.
33
34 [57] S. Byun, B. Ge, H. Song, S.-P. Cho, M. S. Hong, J. Im, I. Chung, *Joule* 2024, 8, 1520.
35
36 [58] Y. Gong, W. Dou, B. Lu, X. Zhang, H. Zhu, P. Ying, Q. Zhang, Y. Liu, Y. Li, X. Huang,
37 M. F. Iqbal, S. Zhang, D. Li, Y. Zhang, H. Wu, G. Tang, *Nat. Commun.* 2024, 15, 4231.
38
39 [59] S. Chandra, U. Bhat, P. Dutta, A. Bhardwaj, R. Datta, K. Biswas, *Adv. Mater.* 2022, 34,
40 2203725.
41
42 [60] V. Taneja, N. Goyal, S. Das, S. Chandra, P. Dutta, N. Ravishankar, K. Biswas, *J. Am.*
43 *Chem. Soc.* 2024, 146, 24716.
44
45 [61] C. Fiedler, Y. Liu, M. Ibáñez, *JoVE* 2024, e66278.
46
47
48
49
50
51
52
53
54
55
56
57
58
59
60

- 1
2
3
4 [62] C. Chang, Y. Liu, S. Ho Lee, M. Chiara Spadaro, K. M. Koskela, T. Kleinhanns, T.
5 Costanzo, J. Arbiol, R. L. Brutchey, M. Ibáñez, *Angew. Chemie Int. Ed.* 2022, 61,
6 e202207002.
7
8
9 [63] C. Xing, Y. Zhang, K. Xiao, X. Han, Y. Liu, B. Nan, M. G. Ramon, K. H. Lim, J. Li, J.
10 Arbiol, B. Poudel, A. Nozariasbmarz, W. Li, M. Ibáñez, A. Cabot, *ACS Nano* 2023, 17,
11 8442.
12
13
14 [64] D. S. Dolzhenkov, H. Zhang, J. Jang, J. S. Son, M. G. Panthani, T. Shibata, S.
15 Chattopadhyay, D. V Talapin, *Science* 2015, 347, 425.
16
17
18 [65] Y. Xiao, L. D. Zhao, *Science* 2020, 367, 1196.
19
20 [66] B. Qin, M. G. Kanatzidis, L.-D. Zhao, *Science* 2024, 386, eadp2444.
21
22 [67] F. Zhang, D. Wu, J. He, *Mater. Lab* 2022, 1, 220011.
23
24 [68] C. Hu, K. Xia, C. Fu, X. B. Zhao, T. Zhu, *Energy Environ. Sci.* 2022, 15, 1406.
25
26
27
28
29
30
31
32
33
34
35
36
37
38
39
40
41
42
43
44
45
46
47
48
49
50
51
52
53
54
55
56
57
58
59
60

Accepted Article
This article has been accepted for publication and undergone full peer review but has not been through the copyediting, typesetting, pagination and proofreading process, which may lead to differences between this version and the Version of Record.

Biographies



Shaoqing Lu is a Ph.D. candidate under the supervision of Prof. Yu Liu at the School of Chemistry and Chemical Engineering, Hefei University of Technology. He received his B.S. in Materials Science and Engineering from the same university. His research focuses on the synthesis and optimization of thermoelectric materials, especially lead-based chalcogenides.



Lulu Huang joined the School of Materials Science and Engineering at Hefei University of Technology in 2021. She received her Ph.D. from the University of Science and Technology of China and spent one year as a joint Ph.D. student at Seoul National University. Her current research focuses on exploring the structure-activity relationships between the physical properties and microscopic components of thermoelectric materials.



Yu Liu is a professor at the School of Chemistry and Chemical Engineering, Hefei University of Technology. He received his Ph.D. from the University of Barcelona in 2018 subsequently carried out postdoctoral research at the Institute of Science and Technology Austria from 2018 to 2021. His research focuses on the bottom-up engineering of chalcogenide nanostructures to develop high-performance thermoelectric materials and devices.

This article has been accepted for publication and undergone full peer review but has not been through the copyediting, typesetting, pagination and proofreading process, which may lead to differences between this version and the Version of Record.

Development of Solution-Processed p-Type Polycrystalline SnSe Thermoelectric Nanomaterials

Shaoqing Lu,^a Lulu Huang,^b Yu Liu^{a,*}

^a School of Chemistry and Chemical Engineering, Hefei University of Technology, 230009, Hefei, China.

^b School of Materials Science and Engineering, Hefei University of Technology, Hefei 230009, China.

* E-mail: yliu@hfut.edu.cn

This article has been accepted for publication and undergone full peer review but has not been through the copyediting, typesetting, pagination and proofreading process, which may lead to differences between this version and the Version of Record.

Accepted Article
FOR Review Only

Abstract: SnSe has emerged as a promising mid-temperature thermoelectric (TE) material, noted for its intrinsically low lattice thermal conductivity and favorable electronic properties. Solution-processing provides a scalable and adaptable approach to synthesizing polycrystalline SnSe, allowing for precise control over nanostructure, defect density, and dopant distribution, which are essential factors in optimizing TE performance. Advances in doping/alloying, defect engineering and surface functionalization have been shown to enhance carrier concentrations, Seebeck coefficients, and reduced lattice thermal conductivity in p-type SnSe, resulting in notable TE efficiency. However, achieving comparable efficiency in solution-processed n-type SnSe remains challenging due to limited electron carrier concentration. In addition, low carrier mobility further limits the TE performance of polycrystalline SnSe at low temperatures. This perspective briefly explores the development of solution-processed SnSe nanostructures, with a focus on ongoing advancements in processing techniques and optimization strategies essential for promoting solution-processed SnSe toward practical TE applications.

Key words: Thermoelectric; Solution processing; Tin selenide

1
2
3
4 Thermolectric (TE) materials enable the direct and reversible conversion of heat into
5
6 electricity, making them highly valuable for applications in clean energy, aerospace technology,
7
8 and solid-state cooling. TE devices consist of multiple p-type and n-type inorganic
9
10 semiconductors, which are arranged electrically in series and thermally in parallel to form an
11
12 all-solid-state module^[1]. The efficiency of TE devices is determined by the figure of merit (zT),
13
14 which integrates the Seebeck coefficient (S), electrical conductivity (σ), and thermal
15
16 conductivity (κ). Achieving high zT values requires a precise balance of these properties,
17
18 thereby enhancing energy conversion efficiency^[2,3].
19
20
21
22
23
24

25 SnSe has become as a promising candidate for medium-temperature TE applications,
26
27 owing to its unique layered structure and excellent TE properties^[4,5]. In 2014, Zhao *et al.* first
28
29 reported the ultralow thermal conductivity and high figure of merit zT in single-crystalline SnSe,
30
31 this material has consistently demonstrated remarkable zT values along specific
32
33 crystallographic directions^[6]. These outstanding properties are primarily attributed to its
34
35 intrinsically low lattice thermal conductivity (κ_L) and favorable electronic characteristics^[7]. The
36
37 application of single-crystal SnSe has been constrained by high production costs and challenges
38
39 in mechanical stability^[4]. Thus, polycrystalline SnSe provides a mechanically robust alternative
40
41 with the potential for scalable production. However, polycrystalline SnSe synthesized via both
42
43 solution-based^[8–30] and solid-state^[31–43] methods often exhibits carrier mobility that is reduced
44
45 by an order of magnitude compared to single crystals (Figure 1a)^[6]. This reduction is primarily
46
47 caused by strong carrier scattering at closely arranged grain boundaries and surface oxidation
48
49 at grain interfaces, which together lead to lower σ , particularly at low temperatures, and higher
50
51
52
53
54
55
56
57
58
59
60

κ compared to SnSe crystals^[4,44]. To enhance the TE performance of polycrystalline SnSe and address existing challenges, strategies including stoichiometry control^[8,9,11,12,16], doping/alloying^[10,13,15,17,18,20,22–26,31–38,40–43], nanocomposites (NCPs) formation^[14,19,21,28,29], and surface oxide removal have been applied^[39,45], leading to significant improvements in zT values for materials produced by both solid-state and solution-processed methods.

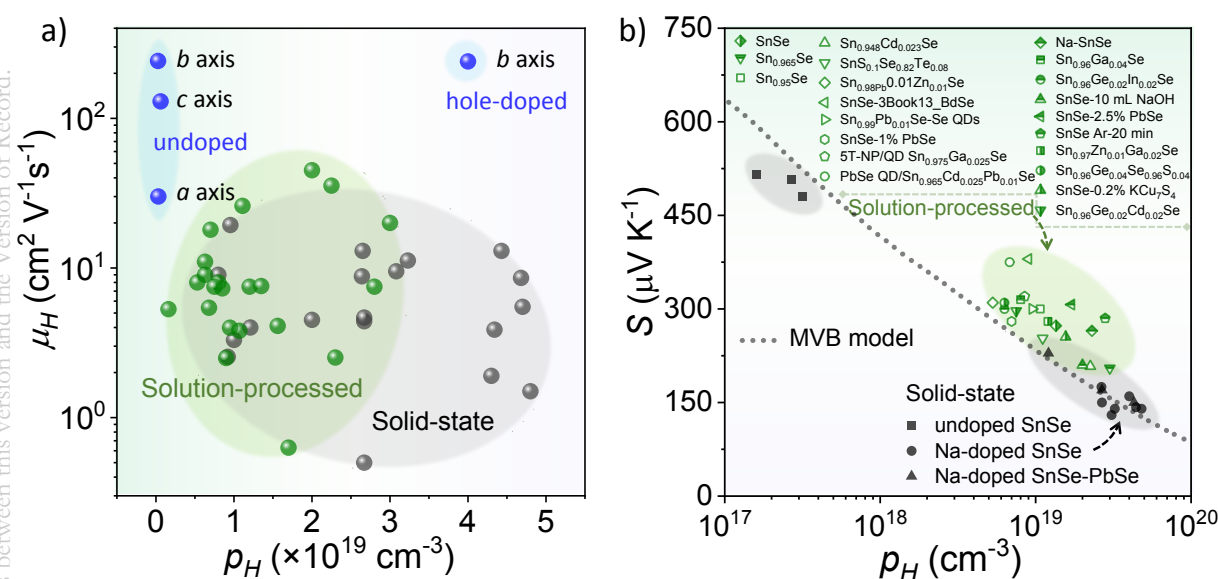


Figure 1. (a) Hall mobility (μ_H) of p-type polycrystalline SnSe as a function of hole concentration (p_H) for solution-processed (green dots)^[8–30], solid-state (gray dots)^[31–43], and single-crystal SnSe (blue dots)^[6,46]. (b) Pisarenko plot at 300 K, with green symbols representing solution-processed materials^[8–22,24–30] and black symbols denoting solid-state synthetic methods^[31,35–40], including single crystals^[6,46]. The dashed line was calculated using a multiple band model^[47].

In comparison to solid-phase methods, solution-processing provides a cost-effective and scalable approach that allows precise control over material morphology, grain size, composition,

1
2
3
4 and crystalline structure, while traditional solid-state synthesis requires high temperatures and
5
6 substantial energy^[1]. The control available in solution-processed SnSe enables the formation of
7
8 specific nanostructural features, *i.e.*, defect engineering, grain boundary construction, and
9
10 optimized dopant distribution, which are essential for improving phonon scattering and thus
11
12 enhancing TE properties, ultimately providing distinct advantages in tailoring overall
13
14 performance. Additionally, this technique allows for the incorporation of various dopants and
15
16 secondary phases, providing a versatile approach for optimizing both carrier concentration and
17
18 mobility^[48]. Therefore, while polycrystalline SnSe-based TE materials prepared by solution-
19
20 processing methods exhibit slightly lower carrier concentrations than those produced by solid-
21
22 state techniques (Figure 1a), the comparable carrier mobility and reduced κ_L contribute to
23
24 enhanced TE performance.
25
26
27
28
29
30

31
32 Initially, SnSe attracted attention as a key p-type IV-VI semiconductor due to its nearly
33
34 optimal bandgap for photovoltaic applications, before being recognized as a promising TE
35
36 material, with synthetic approaches primarily using colloidal methods that, despite their ability
37
38 to produce high-quality SnSe nanocrystals (NCs) in various morphologies including nanostars,
39
40 nanowires, nanoflowers, and nanosheets, face significant limitations in scalability and practical
41
42 application resulting from their reliance on TOP-Se, a highly toxic and expensive
43
44 trioctylphosphine-based precursor^[49–51]. This limitation has directed researchers toward
45
46 hydrothermal/solvothermal^[8,9,21,23,24,26,27,29,30,10–12,15–18,20], and aqueous solution-based synthesis
47
48 methods^[13,14,19,22,25,28,52], which provide safer, more economically feasible alternatives for large-
49
50 scale production by reducing the dependence on toxic reagents, thereby facilitating the scalable
51
52
53
54
55
56
57
58
59
60

development of TE materials. The production of surfactant-free SnSe nanomaterials typically involves polar solvents, such as water or ethylene glycol, in hydrothermal/solvothermal methods, or is carried out in aqueous solution-based methods at atmospheric pressure in boiling water. These reactions commonly employ sodium-containing compounds, including NaBH_4 , NaOH , and Na_2SeO_3 , *etc.*, as redox agents and acid/base additives^[8–30]. Compared to conventional hydrothermal and solvothermal methods, aqueous solution-based approaches present notable advantages by minimizing the reliance on specialized reaction vessels and conditions, enhancing economic efficiency, and providing significant potential for large-scale production.

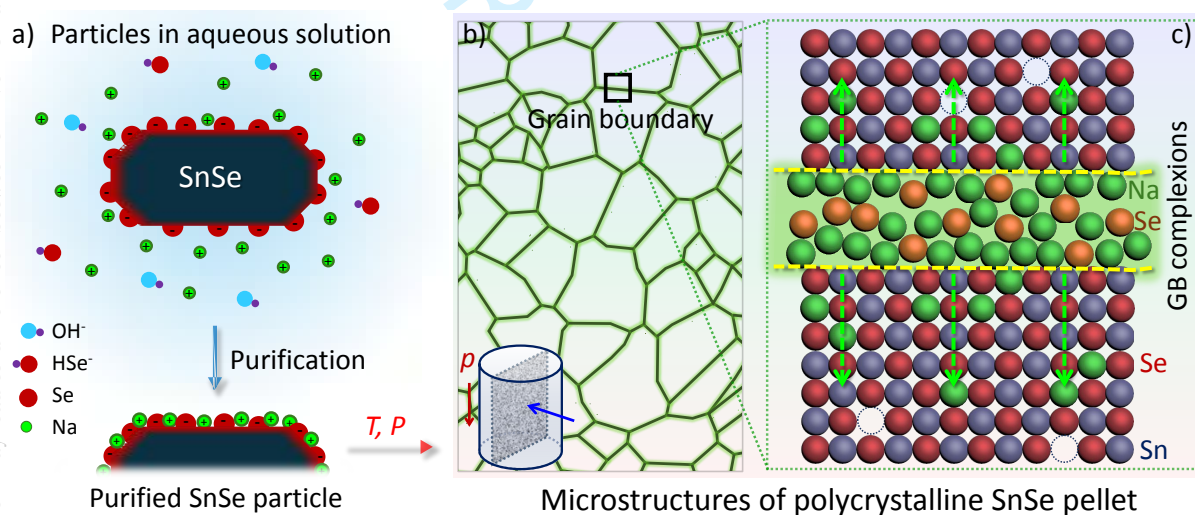


Figure 2. (a) Schematic representation of a SnSe particle in aqueous solution, with Na^+ ions adsorbed to maintain charge neutrality after purification^[13]. (b) Diagram of the grain boundary interface in aqueous-synthesized SnSe after thermal annealing and sintering. (c) Enlarged view of the grain boundary (GB), showing the complexes and atomic diffusion mechanisms within the matrix of the system.

1
2
3
4 Surfactant-free SnSe particles synthesized via aqueous solution methods exhibit high σ
5
6 and S after consolidation, while maintaining relatively low κ_L , a combination that enables
7
8 superior TE performance without requiring intentional doping. Compared to SnSe produced via
9
10 conventional solid-state methods, this method yields samples with significantly high carrier
11
12 concentrations ($>2 \times 10^{19} \text{ cm}^{-3}$), a characteristic attributed in previous studies not solely to
13
14 intrinsic Sn vacancies^[13,53]. The aqueous solution synthesis process involves alternating
15
16 purification steps with solvents of different polarities, such as water and ethanol, which are
17
18 essential for controlling composition and optimizing performance. Our recent studies have
19
20 thoroughly examined the critical chemical processing steps involved in the solution-based
21
22 synthesis of SnSe, including particle synthesis, purification, annealing, and consolidation^[53].
23
24 During these steps, residual Na^+ ions, electrostatically adsorbed onto the negatively charged
25
26 surfaces of SnSe particles, remain partially unremovable through purification and subsequently
27
28 combine with excess Se on the particle surface to form Na_2Se_x phases^[13]. Upon annealing in
29
30 forming gas (95% N_2 + 5% H_2) and subsequent consolidation, these low-melting Na_2Se_x phases
31
32 facilitate microstructural optimization^[54,55], significantly enhancing TE transport properties by
33
34 increasing carrier concentration and enhancing the S through the energy-filtering effect at grain
35
36 boundary barriers. Furthermore, the Pisarenko plot reveals that most solution-processed SnSe
37
38 samples (green symbols) exhibit S values exceeding the expected values, a trend not observed
39
40 in Na-doped solid-state synthesized SnSe samples (black symbols, including single crystals),
41
42 as shown in Figure 1b. Na^+ ions ultimately stabilize within bulk SnSe in two distinct forms: i)
43
44 as partial substitutes for Sn^{2+} within the lattice, acting as p-type dopants; and ii) at grain
45
46
47
48
49
50
51
52
53
54
55
56
57
58
59
60

1
2
3
4 boundaries and defects, accumulating during sintering to form Na-enriched interfacial
5
6 complexions or precipitates at grain boundaries (Figure 2). Therefore, the influence of surface
7
8 adsorbates requires careful consideration, especially when alkali metal salts or hydroxides (such
9
10 as Li⁺ or K⁺, in addition to Na⁺) are employed as reactants in solution-based synthesis. Precise
11
12 control over the purification, thermal annealing treatment, and sintering processes of SnSe
13
14 particles is crucial, accompanied by detailed documentation of these steps in the experimental
15
16 section to ensure reproducibility^[53].
17
18
19

20
21
22 While the solution-processed p-type SnSe bulk materials have achieved ideal carrier
23
24 concentration levels (10^{19} cm^{-3}) and exhibit superior TE performance, it is notable that n-type
25
26 SnSe synthesized via aqueous or other solution-based methods shows considerably lower TE
27
28 efficiency in comparison to its p-type SnSe. Despite increasing the content of n-type dopants,
29
30 achieving a substantial enhancement in electron carrier concentration remains challenging^[22,56].
31
32
33

34
35 We believe this is correlated to the fact that all synthetic methods use of alkali metal Na salts
36
37 in the preparation of SnSe particles, where the presence of Na induces a pinning effect when n-
38
39 type dopants are introduced and is further supported by the fact that all reported high-
40
41 performance n-type polycrystalline SnSe materials ($zT > 2$) have been synthesized through solid-
42
43 state methods^[57-60]. Therefore, to develop high-performance n-type polycrystalline SnSe
44
45 through solution-processed methods, avoiding the use of alkali metal salts or alkali hydroxides
46
47 is recommended, with alternative reagents, *e.g.*, tetramethylammonium salts and ascorbic acid,
48
49 serving as potential substitutes.
50
51
52
53

54
55
56 Moreover, we suggest that for p-type SnSe particles synthesized via aqueous solution
57
58
59
60

methods with alkali metal compounds as reactants, efforts to improve electrical transport properties through doping/alloying are often ineffective, with these strategies potentially further reducing the already low carrier mobility of the polycrystalline SnSe, leading to an additional decrease in σ , especially at low temperatures. For example, during the alloying process where surfactant-free SnSe particles are combined with colloidal PbSe NCs to form SnSe-PbSe NCPs some Na^+ ions electrostatically adsorbed on the surfaces of the SnSe particles interact with the oleate capping ligands on PbSe NCs, forming Na-oleate, which is subsequently removed through particle purification^[14].

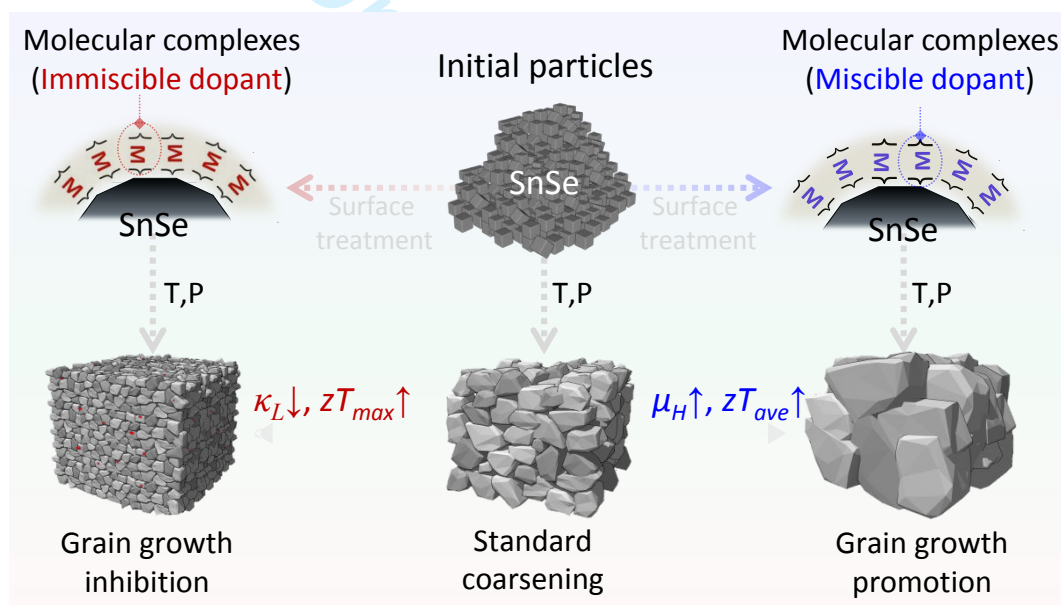


Figure 3. Schematic of crystal domain growth during the annealing and consolidation of SnSe particles under conditions without and with different types of molecular complexes.

The surface functionalization of SnSe particles with CdSe molecular complexes, prepared in an “amine-thiol” solution, results in SnSe-CdSe NCPs in which CdSe remains insoluble within the SnSe matrix across the entire operating temperature range. CdSe nanoprecipitates

1
2
3
4 are uniformly distributed within the SnSe matrix, creating a high density of grain boundaries
5
6 through a Zener pinning effect that inhibits significant grain growth in SnSe-CdSe samples
7
8 during thermal processing, thereby preserving the dimensional advantages characteristic of
9
10 low-dimensional nanostructured TE materials^[28,61]. With coordinated control of dislocations
11
12 and multiscale defects, this structure effectively reduces the κ_L of the NCPs. Simultaneously,
13
14 the consistent level of unavoidable Na impurities during the surface treatment of polycrystalline
15
16 SnSe maintains electrical properties, significantly enhancing its high-temperature TE
17
18 performance, yielding a zT of 2.2 at 786 K. This approach is particularly effective for systems
19
20 with high carrier concentrations, such as SnTe, Cu_{2-x}Te and Ag_2Se -based materials^[62,63], that
21
22 seek to maximize TE performance (zT_{max}) in the mid-to-high temperature range by reducing κ_L .
23
24 For materials requiring a high average thermoelectric figure of merit (zT_{ave}) across low-
25
26 temperature ranges, enhancing carrier mobility through grain boundary engineering and
27
28 optimized doping mechanisms is essential, as is identifying molecular complexes compatible
29
30 with the SnSe matrix that effectively function as “solders” mutually soluble with the matrix.^[64]
31
32 These “solder” complexes, when applied to the SnSe particle surface, facilitate atomic diffusion
33
34 into the grains during high-temperature treatment, thereby promoting solid solution formation,
35
36 accelerating grain boundary migration, and inducing grain growth. This process reduces grain
37
38 boundary barriers and enhances carrier mobility in polycrystalline SnSe at low-temperature
39
40 range (Figure 3)^[2,65–68]. However, identifying compatible systems and optimizing post-
41
42 treatment conditions based on the phase diagrams of SnSe and related compounds remains
43
44 challenging.
45
46
47
48
49
50
51
52
53
54
55
56
57
58
59
60

1
2
3
4 In this perspective, the strategies discussed above provide valuable insights into the
5
6 transport mechanisms of TE materials and open new avenues for the controlled synthesis of
7
8 advanced polycrystalline SnSe-based TE nanostructures. Solution-processed SnSe
9
10 demonstrates significant potential for high TE performance through defect and surface
11
12 engineering; however, further optimization remains crucial for advancing solution-processed
13
14 SnSe toward practical applications, with key improvements including refining solution-
15
16 processing conditions to achieve greater reproducibility, enhancing material stability against
17
18 oxidation, and optimizing carrier mobility.
19
20
21
22
23
24
25
26
27

28 **Acknowledgements**

29
30
31 Y.L. acknowledges funding from the National Natural Science Foundation of China (NSFC)
32
33 (Grants No. 22209034), the Innovation and Entrepreneurship Project of Overseas Returnees in
34
35 Anhui Province (Grant No. 2022LCX002) and the Fundamental Research Funds for the Central
36
37 Universities (JZ2024HGTA0179). L.H. acknowledges the Fundamental Research Funds for the
38
39 Central Universities (JZ2023HGTA0179).
40
41
42
43
44

45 **Conflict of interest**

46
47
48 The authors declare no conflict of interest.
49
50

51 **REFERENCES**

- 52
53 [1] S. Ortega, M. Ibáñez, Y. Liu, Y. Zhang, M. V. Kovalenko, D. Cadavid, A. Cabot, *Chem.*
54
55 *Soc. Rev.* 2017, 46, 3510.
56
57 [2] B. Qin, L.D. Zhao, *Mater. Lab* 2022, 1, 220004.
58
59
60

- [3] Y. Xiao, *Mater. Lab* 2022, 1, 220025.
- [4] L. D. Zhao, C. Chang, G. Tan, M. G. Kanatzidis, *Energy Environ. Sci.* 2016, 9, 3044.
- [5] D. Liu, B. Qin, L.D. Zhao, *Mater. Lab* 2022, 1, 220006.
- [6] L. D. Zhao, S. H. Lo, Y. Zhang, H. Sun, G. Tan, C. Uher, C. Wolverton, V. P. Dravid, M. G. Kanatzidis, *Nature* 2014, 508, 373.
- [7] Y. Xiao, C. Chang, Y. Pei, D. Wu, K. Peng, X. Zhou, S. Gong, J. He, Y. Zhang, Z. Zeng, L.D. Zhao, *Phys. Rev. B* 2016, 94, 125203.
- [8] W. Wei, C. Chang, T. Yang, J. Liu, H. Tang, J. Zhang, Y. Li, F. Xu, Z. Zhang, J.-F. Li, G. Tang, *J. Am. Chem. Soc.* 2017, 140, 499.
- [9] X. Shi, Z. G. Chen, W. Liu, L. Yang, M. Hong, R. Moshwan, L. Huang, J. Zou, *Energy Storage Mater.* 2018, 10, 130.
- [10] Y. Gong, S. Zhang, Y. Hou, S. Li, C. Wang, W. Xiong, Q. Zhang, X. Miao, J. Liu, Y. Cao, *ACS Nano* 2022, 17, 801.
- [11] X. Shi, W. Liu, A. Wu, V. T. Nguyen, H. Gao, Q. Sun, R. Moshwan, J. Zou, Z. Chen, *InfoMat* 2020, 2, 1201.
- [12] X.-L. Shi, W.-D. Liu, M. Li, Q. Sun, S.-D. Xu, D. Du, J. Zou, Z.-G. Chen, *Adv. Energy Mater.* 2022, 12, 2200670.
- [13] Y. Liu, M. Calcabrini, Y. Yu, A. Genç, C. Chang, T. Costanzo, T. Kleinhanns, S. Lee, J. Llorca, O. Cojocar-Mirédin, M. Ibáñez, *Adv. Mater.* 2021, 33, 2106858.
- [14] Y. Liu, S. Lee, C. Fiedler, M. Chiara Spadaro, C. Chang, M. Li, M. Hong, J. Arbiol, M. Ibáñez, *Chem. Eng. J.* 2024, 490, 151405.
- [15] S. Li, X. Lou, B. Zou, Y. Hou, J. Zhang, D. Li, J. Fang, T. Feng, D. Zhang, Y. Liu, *Mater. Today Phys.* 2021, 21, 100542.
- [16] C. Wu, X. Shi, M. Li, Z. Zheng, L. Zhu, K. Huang, W. Liu, P. Yuan, L. Cheng, Z. Chen, *Adv. Funct. Mater.* 2024, 34, 2402317.
- [17] S. Li, Y. Hou, D. Li, B. Zou, Q. Zhang, Y. Cao, G. Tang, *J. Mater. Chem. A* 2022, 10, 12429.
- [18] Y. Gong, P. Ying, Q. Zhang, Y. Liu, X. Huang, W. Dou, Y. Zhang, D. Li, D. Zhang, T. Feng, *Energy Environ. Sci.* 2024, 17, 1612.

- 1
2
3
4 [19] X. Liu, Y. Chen, H. Wang, S. Liu, B. Zhang, X. Lu, G. Wang, G. Han, X. Chen, X. Zhou,
5 *ACS Appl. Mater. Interfaces* 2024, 16, 2240.
6
7 [20] X. Lou, S. Li, X. Chen, Q. Zhang, H. Deng, J. Zhang, D. Li, X. Zhang, Y. Zhang, H.
8 Zeng, G. Tang, *ACS Nano* 2021, 15, 8204.
9
10 [21] W. Dou, Y. Gong, X. Huang, Y. Li, Q. Zhang, Y. Liu, Q. Xia, Q. Jian, D. Xiang, D. Li,
11 D. Zhang, S. Zhang, P. Ying, G. Tang, *Small* 2024, 20, 2311153.
12
13 [22] X. Li, C. Chen, W. Xue, S. Li, F. Cao, Y. Chen, J. He, J. Sui, X. Liu, Y. Wang, Q. Zhang,
14 *Inorg. Chem.* 2018, 57, 13800.
15
16 [23] Z.-C. Wang, X.-D. Jiang, Y.-X. Duan, X. Wang, Z.-H. Ge, J.-M. Cai, X.-M. Cai, H.-L.
17 Tan, *J. Eur. Ceram. Soc.* 2024, 44, 1636.
18
19 [24] X. Shi, A. Wu, T. Feng, K. Zheng, W. Liu, Q. Sun, M. Hong, S. T. Pantelides, Z.-G.
20 Chen, J. Zou, *Adv. Energy Mater.* 2019, 9, 1803242.
21
22 [25] L. Huang, G. Han, B. Zhang, D. H. Gregory, *J. Mater. Chem. C* 2019, 7, 7572.
23
24 [26] J. J. Liu, P. Wang, M. Wang, R. Xu, J. Zhang, J. J. Liu, D. Li, N. Liang, Y. Du, G. Chen,
25 G. Tang, *Nano Energy* 2018, 53, 683.
26
27 [27] R. Xu, L. Huang, J. Zhang, D. Li, J. Liu, J. Liu, J. Fang, M. Wang, G. Tang, *J. Mater.*
28 *Chem. A* 2019, 7, 15757.
29
30 [28] Y. Liu, M. Calcabrini, Y. Yu, S. Lee, C. Chang, J. David, T. Ghosh, M. C. Spadaro, C.
31 Xie, O. Cojocar-Mirédin, J. Arbiol, M. Ibáñez, *ACS Nano* 2022, 16, 78.
32
33 [29] G. Tang, W. Wei, J. Zhang, Y. Li, X. Wang, G. Xu, C. Chang, Z. Wang, Y. Du, L. D.
34 Zhao, *J. Am. Chem. Soc.* 2016, 138, 13647.
35
36 [30] S. Li, Y. Hou, S. Zhang, Y. Gong, S. Siddique, D. Li, J. Fang, P. Nan, B. Ge, G. Tang,
37 *Chem. Eng. J.* 2023, 451, 138637.
38
39 [31] T. R. Wei, G. Tan, X. Zhang, C. F. Wu, J. F. Li, V. P. Dravid, G. J. Snyder, M. G.
40 Kanatzidis, *J. Am. Chem. Soc.* 2016, 138, 8875.
41
42 [32] T. R. Wei, C. F. Wu, X. Zhang, Q. Tan, L. Sun, Y. Pan, J. F. Li, *Phys. Chem. Chem.*
43 *Phys.* 2015, 17, 30102.
44
45 [33] C.-C. Lin, R. Lydia, J. Hyun Yun, H. Seong Lee, J. Soo Rhyee, *Chem. Mater.* 2017, 29,
46 5344.
47
48
49
50
51
52
53
54
55
56
57
58
59
60

- [34] B. Su, Z. Han, Y. Jiang, H.-L. Zhuang, J. Yu, J. Pei, H. Hu, J.-W. Li, Y.-X. He, B.-P. Zhang, J.-F. Li, *Adv. Funct. Mater.* 2023, 33, 2301971.
- [35] E. K. Chere, Q. Zhang, K. Dahal, F. Cao, J. Mao, Z. Ren, *J. Mater. Chem. A* 2016, 4, 1848.
- [36] Y. Luo, S. Cai, X. Hua, H. Chen, Q. Liang, C. Du, Y. Zheng, J. Shen, J. Xu, C. Wolverton, V. P. Dravid, Q. Yan, M. G. Kanatzidis, *Adv. Energy Mater.* 2019, 9, 1803072.
- [37] B. Cai, J. Li, H. Sun, P. Zhao, F. Yu, L. Zhang, D. Yu, Y. Tian, B. Xu, *J. Alloys Compd.* 2017, 727, 1014.
- [38] Z. H. Ge, D. Song, X. Chong, F. Zheng, L. Jin, X. Qian, L. Zheng, R. E. Dunin-Borkowski, P. Qin, J. Feng, L. D. Zhao, *J. Am. Chem. Soc.* 2017, 139, 9714.
- [39] Y. K. Lee, Z. Luo, S. P. Cho, M. G. Kanatzidis, I. Chung, *Joule* 2019, 3, 719.
- [40] Q. Zhao, D. Wang, B. Qin, G. Wang, Y. Qiu, L. D. Zhao, *J. Solid State Chem.* 2019, 273, 85.
- [41] Y. X. Chen, Z. H. Ge, M. Yin, D. Feng, X. Q. Huang, W. Zhao, J. He, *Adv. Funct. Mater.* 2016, 26, 6836.
- [42] S. Liang, J. Xu, J. G. Noudem, H. Wang, X. Tan, G.-Q. Liu, H. Shao, B. Yu, S. Yue, J. Jiang, *J. Mater. Chem. A* 2018, 6, 23730.
- [43] Q. Zhao, B. Qin, D. Wang, Y. Qiu, L.-D. Zhao, *ACS Appl. Energy Mater.* 2019, 3, 2049.
- [44] A. K. Munirathnappa, H. Lee, I. Chung, *Mater. Lab* 2023, 2, 220056.
- [45] C. Zhou, Y. K. Lee, Y. Yu, S. Byun, Z.-Z. Luo, H. Lee, B. Ge, Y.-L. Lee, X. Chen, J. Y. Lee, O. Cojocar-Mirédin, H. Chang, J. Im, S.-P. Cho, M. Wuttig, V. P. Dravid, M. G. Kanatzidis, I. Chung, *Nat. Mater.* 2021, 20, 1378.
- [46] L.-D. Zhao, G. Tan, S. Hao, J. He, Y. Pei, H. Chi, H. Wang, S. Gong, H. Xu, V. P. Dravid, C. Uher, G. J. Snyder, C. Wolverton, M. G. Kanatzidis, *Science* 2016, 351, 141.
- [47] G. Shi, E. Kioupakis, *J. Appl. Phys.* 2015, 117, 065103.
- [48] C. Fiedler, T. Kleinhanns, M. Garcia, S. Lee, M. Calcabrini, M. Ibáñez, *Chem. Mater.* 2022, 34, 8471.
- [49] L. Li, Z. Chen, Y. Hu, X. Wang, T. Zhang, W. Chen, Q. Wang, *J. Am. Chem. Soc.* 2013, 135, 1213.

- 1
2
3
4 [50] X. Liu, Y. Li, B. Zhou, X. Wang, A. N. Cartwright, M. T. Swihart, *Chem. Mater.* 2014,
5 26, 3515.
6
7 [51] S. Liu, X. Guo, M. Li, W. H. Zhang, X. Liu, C. Li, *Angew. Chemie Int. Ed.* 2011, 50,
8 12050.
9
10 [52] G. Han, S. R. Popuri, H. F. Greer, J. W. G. Bos, W. Zhou, A. R. Knox, A. Montecucco,
11 J. Siviter, E. A. Man, M. MacAuley, D. J. Paul, W. G. Li, M. C. Paul, M. Gao, T. Sweet,
12 R. Freer, F. Azough, H. Baig, N. Sellami, T. K. Mallick, D. H. Gregory, *Angew. Chemie*
13 *Int. Ed.* 2016, 55, 6433.
14
15 [53] C. Fiedler, M. Calcabrini, Y. Liu, M. Ibáñez, *Angew. Chemie Int. Ed.* 2024, 63,
16 e202402628.
17
18 [54] J. Sangster, A. D. Pelton, *J. Phase Equilib.* 1997, 18, 185.
19
20 [55] S.-J. L. Kang, *Sintering: Densification, Grain Growth, and Microstructure*, Butterworth–
21 Heinemann, Oxford 2005.
22
23 [56] G. Han, S. R. Popuri, H. F. Greer, L. F. Llin, J.-W. G. Bos, W. Zhou, D. J. Paul, H.
24 Ménard, A. R. Knox, A. Montecucco, J. Siviter, E. A. Man, W. Li, M. C. Paul, M. Gao,
25 T. Sweet, R. Freer, F. Azough, H. Baig, T. K. Mallick, D. H. Gregory, *Adv. Energy Mater.*
26 2017, 7, 1602328.
27
28 [57] S. Byun, B. Ge, H. Song, S.-P. Cho, M. S. Hong, J. Im, I. Chung, *Joule* 2024, 8, 1520.
29
30 [58] Y. Gong, W. Dou, B. Lu, X. Zhang, H. Zhu, P. Ying, Q. Zhang, Y. Liu, Y. Li, X. Huang,
31 M. F. Iqbal, S. Zhang, D. Li, Y. Zhang, H. Wu, G. Tang, *Nat. Commun.* 2024, 15, 4231.
32
33 [59] S. Chandra, U. Bhat, P. Dutta, A. Bhardwaj, R. Datta, K. Biswas, *Adv. Mater.* 2022, 34,
34 2203725.
35
36 [60] V. Taneja, N. Goyal, S. Das, S. Chandra, P. Dutta, N. Ravishankar, K. Biswas, *J. Am.*
37 *Chem. Soc.* 2024, 146, 24716.
38
39 [61] C. Fiedler, Y. Liu, M. Ibáñez, *JoVE* 2024, e66278.
40
41 [62] C. Chang, Y. Liu, S. Ho Lee, M. Chiara Spadaro, K. M. Koskela, T. Kleinhanns, T.
42 Costanzo, J. Arbiol, R. L. Brutchey, M. Ibáñez, *Angew. Chemie Int. Ed.* 2022, 61,
43 e202207002.
44
45 [63] C. Xing, Y. Zhang, K. Xiao, X. Han, Y. Liu, B. Nan, M. G. Ramon, K. H. Lim, J. Li, J.

Arbiol, B. Poudel, A. Nozariasbmarz, W. Li, M. Ibáñez, A. Cabot, *ACS Nano* 2023, 17, 8442.

[64] D. S. Dolzhenkov, H. Zhang, J. Jang, J. S. Son, M. G. Panthani, T. Shibata, S. Chattopadhyay, D. V Talapin, *Science* 2015, 347, 425.

[65] Y. Xiao, L. D. Zhao, *Science* 2020, 367, 1196.

[66] B. Qin, M. G. Kanatzidis, L.-D. Zhao, *Science* 2024, 386, eadp2444.

[67] F. Zhang, D. Wu, J. He, *Mater. Lab* 2022, 1, 220011.

[68] C. Hu, K. Xia, C. Fu, X. B. Zhao, T. Zhu, *Energy Environ. Sci.* 2022, 15, 1406.

Accepted Article
This article has been accepted for publication and undergone full peer review but has not been through the copyediting, typesetting, pagination and proofreading process, which may lead to differences between this version and the Version of Record.

For Review Only

Biographies



Shaoqing Lu is a Ph.D. candidate under the supervision of Prof. Yu Liu at the School of Chemistry and Chemical Engineering, Hefei University of Technology. He received his B.S. in Materials Science and Engineering from the same university. His research focuses on the synthesis and optimization of thermoelectric materials, especially lead-based chalcogenides.



Lulu Huang joined the School of Materials Science and Engineering at Hefei University of Technology in 2021. She received her Ph.D. from the University of Science and Technology of China and spent one year as a joint Ph.D. student at Seoul National University. Her current research focuses on exploring the structure-activity relationships between the physical properties and microscopic components of thermoelectric materials.



Yu Liu is a professor at the School of Chemistry and Chemical Engineering, Hefei University of Technology. He received his Ph.D. from the University of Barcelona in 2018 subsequently carried out postdoctoral research at the Institute of Science and Technology Austria from 2018 to 2021. His research focuses on the bottom-up engineering of chalcogenide nanostructures to develop high-performance thermoelectric materials and devices.

This article has been accepted for publication and undergone full peer review but has not been through the copyediting, typesetting, pagination and proofreading process, which may lead to differences between this version and the Version of Record.

Accepted Article